

Three-sphere low-Reynolds-number swimmer with muscle-like arms

ALESSANDRO MONTINO¹ AND ANTONIO DESIMONE^{1,2,*}

¹*GSSI - Gran Sasso Science Institute, viale Francesco Crispi 7, 67100 L'Aquila, Italy.*

²*SISSA - International School for Advanced Studies, via Bonomea 265, 34136 Trieste, Italy.*

March 2, 2022

Abstract

The three-sphere swimmer by Najafi and Golestanian is composed of three spheres connected by two arms. The authors of this model studied in detail the case in which the swimmer can generate periodic shape changes by controlling the lengths of the two arms. Here we study a variation of the model in which the geometry of the shape change is not known a priori, because the swimmer is not able of directly controlling the lengths of the arms. Our study is motivated by the fact that real swimmers are not capable of directly controlling their shape. The arms of our three-sphere swimmer are constructed according to Hill's model of muscular contraction. The swimmer is only able to control the forces developed in the active components of the muscle-like arms. The two shape parameters and the forces acting through the two arms evolve according to a system of ODEs. After giving a mathematical formulation of the problem, we study the qualitative properties of the solutions and compute analytically their leading order approximation. Then we present the results of some numerical simulations which are in good agreement with our theoretical predictions. Finally, we study some optimization problems. Our results can help to gain insight into the mechanisms governing locomotion of biological swimmers.

Introduction

The three-sphere swimmer by Najafi and Golestanian [1, 2] is a cornerstone in the literature on low Reynolds number swimming. It is composed of three spheres connected by two arms. The presence of two shape parameters (the

*Corresponding author – e-mail address: desimone@sissa.it – phone: +39 040 3787 455

lengths of the two arms) allows to perform periodic shape changes which are not invariant under time reversal. This is the key to beat Purcell's famous *scallop theorem* [3], which says that low Reynolds number swimmers cannot achieve locomotion through a reciprocal shape change. Another famous example of low Reynolds number swimmer with two shape parameters is the three-link swimmer by Purcell [3]. These two model swimmers have been studied extensively (see for example [4–13]).

In the works [1, 2] the authors study a three-sphere swimmer which is able to perform periodic shape changes by controlling the lengths of the two arms. Real swimmers however are not capable of directly controlling their shape. Their shape change is generated by a complex interplay between different elements: forces generated by the swimmer through internal mechanisms, elastic properties of the swimmer's body, and forces due to interactions with the surrounding viscous fluid. The swimmer is able to control only the first of these components. For this reason it is interesting to study minimal swimmers which are not capable of directly controlling their shape. An interesting work going in this direction is [14], in which the authors consider a three-sphere swimmer whose arms can generate forces thanks to a system of molecular motors and elastic elements. Another possibility is to assume that one of the two shape parameters can be controlled while the other one is driven by a passive elastic spring. This was done in [15] for the three-link swimmer and in [16] for the three-sphere swimmer.

In the present work we study a three-sphere swimmer whose arms are viscoelastic structures constructed according to Hill's active state muscle model. This model, which is very useful for computing the mechanical behaviour of muscles, includes passive elastic elements, a mechanism of viscous damping, and an active component. The swimmer is able to control the force generated by the active component. The geometry of the shape change is not known a priori and will have to be computed by solving a system of ODEs. In the first section we introduce our model and derive the ODEs governing the system. In the second section we study the qualitative properties of solutions, compute analytically the leading order term of their asymptotic expansion, present the results of numerical simulations, and study some optimization problems. In the third section we study a variation of our model, in which one of the two muscle-like arms is replaced by a passive elastic spring.

1 Problem formulation

The aim of this section is to introduce the three-sphere swimmer with muscle-like arms and to obtain a system of ODEs governing its dynamics. In the first subsection we fix the notations and recall some basic facts about the three-sphere swimmer. In the second subsection we assume that the forces acting through the two arms are known functions of time and shape and obtain the equations governing the evolution of the two shape parameters. In the third subsection we model the arms according to Hill's muscle model and obtain a system of ODEs governing the forces acting across each arm, the shape of the

swimmer and its displacement. In the fourth subsection we write the problem in non-dimensional form. In the fifth and last subsection we consider a variation of the problem in which one of the two muscle-like arms is replaced by a passive elastic spring.

1.1 Three-sphere swimmer

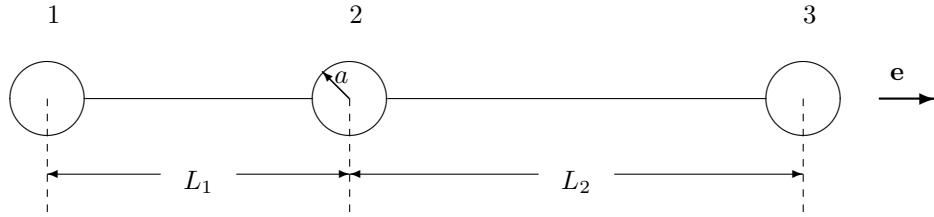


Figure 1: The three-sphere low Reynolds number swimmer.

Let us consider a three-sphere swimmer as in Figure 1. Let a be the radius of the spheres, and L_1, L_2 the lengths of the two arms. We indicate with μ the dynamic viscosity of the fluid and with v_i and f_i respectively the velocity of sphere i and the force that this sphere exerts on the fluid, projected on the unit vector \mathbf{e} . By using the Oseen tensor and the approximation $\frac{a}{L_i} \ll 1$ we obtain the following linear relations between forces and velocities

$$v_1 = \frac{f_1}{6\pi\mu a} + \frac{f_2}{4\pi\mu L_1} + \frac{f_3}{4\pi\mu(L_1 + L_2)}, \quad (1)$$

$$v_2 = \frac{f_1}{4\pi\mu L_1} + \frac{f_2}{6\pi\mu a} + \frac{f_3}{4\pi\mu L_2}, \quad (2)$$

$$v_3 = \frac{f_1}{4\pi\mu(L_1 + L_2)} + \frac{f_2}{4\pi\mu L_2} + \frac{f_3}{6\pi\mu a}. \quad (3)$$

Due to Newton's third law of motion, the force exerted by the fluid on the i -th sphere is $-f_i$. Therefore the force balance equation for the swimmer is

$$f_1 + f_2 + f_3 = 0. \quad (4)$$

The geometry of the system implies the following kinematic relations

$$\dot{L}_1 = v_2 - v_1, \quad (5)$$

$$\dot{L}_2 = v_3 - v_2. \quad (6)$$

Let us indicate with x_i the position of the i -th sphere on axis corresponding to the unit vector \mathbf{e} . We indicate with x the mean point of the three spheres, namely,

$$x := \frac{1}{3}(x_1 + x_2 + x_3). \quad (7)$$

The translational velocity of the swimmer is the velocity of the point x . Obviously

$$\dot{x} = \frac{1}{3}(v_1 + v_2 + v_3). \quad (8)$$

Using equations (1)-(4) we can show that

$$\dot{x} = \left(\frac{1}{L_1 + L_2} - \frac{1}{L_2} \right) \frac{f_1}{12\pi\mu} + \left(\frac{1}{L_1 + L_2} - \frac{1}{L_1} \right) \frac{f_3}{12\pi\mu}. \quad (9)$$

Now we can use equations (1)-(6) to express f_1 and f_3 in terms of $L_1, L_2, \dot{L}_1, \dot{L}_2$. If we plug the resulting expressions into equation (9) and keep only the leading order terms in a/L_j we obtain

$$\dot{x} = \frac{a}{6} \left[\left(\frac{\dot{L}_2 - \dot{L}_1}{L_2 + L_1} \right) + 2 \left(\frac{\dot{L}_1}{L_2} - \frac{\dot{L}_2}{L_1} \right) + \frac{\dot{L}_2}{L_2} - \frac{\dot{L}_1}{L_1} \right]. \quad (10)$$

Suppose that L_1 and L_2 are periodic functions. In this case the terms \dot{L}_j/L_j average to zero in a full swimming cycle, because they are derivatives of $\log(L_j)$. If we neglect these terms we obtain the following formula

$$\dot{x} = \frac{a}{6} \left[\left(\frac{\dot{L}_2 - \dot{L}_1}{L_2 + L_1} \right) + 2 \left(\frac{\dot{L}_1}{L_2} - \frac{\dot{L}_2}{L_1} \right) \right], \quad (11)$$

which can be used instead of (10) to compute the net displacement in one period when the swimmer performs a periodic shape change.

Now we consider the case of small deformations

$$\begin{cases} L_1 = l_1 + U_1 \\ L_2 = l_2 + U_2 \\ U_i/l_j \ll 1. \end{cases} \quad (12)$$

We assume that the deformations are periodic with period T . We would like to compute the net displacement in one period to leading order in the amplitude of deformations. Let us set $l := l_1 + l_2$. l is the body length of the swimmer. If we expand equation (11) and retain only the leading order terms in U_i/l_j we get

$$\dot{\xi} = \frac{a}{6} \left[\frac{\dot{U}_2 - \dot{U}_1}{l_1 + l_2} - \frac{(\dot{U}_2 - \dot{U}_1)(U_1 + U_2)}{(l_1 + l_2)^2} + \frac{2\dot{U}_1}{l_2} - \frac{2\dot{U}_1 U_2}{l_2^2} - \frac{2\dot{U}_2}{l_1} + \frac{2\dot{U}_2 U_1}{l_1^2} \right]. \quad (13)$$

The terms $\dot{U}_j, \dot{U}_j U_j, \dot{U}_1 U_2 + U_1 \dot{U}_2$ give zero when integrated between 0 and T . So the net displacement in one period $l\Delta x$ is given, to leading order in U_i/l_j , by the following formula

$$l\Delta x = \frac{a}{6} \left[\frac{1}{l_1^2} + \frac{1}{l_2^2} - \frac{1}{(l_1 + l_2)^2} \right] \int_0^T (U_1 \dot{U}_2 - \dot{U}_1 U_2) dt. \quad (14)$$

1.2 TSS with assigned tensions

Let us indicate with T_1 and T_2 the tension on the tail rod and on the front rod respectively. We assume that T_1 and T_2 are known functions of time and shape, namely, $T_i = T_i(t, L_1, L_2)$, $i = 1, 2$. The equations of force balance for the three spheres are

$$-f_1 + T_1 = 0 \quad (15)$$

$$-f_2 - T_1 + T_2 = 0 \quad (16)$$

$$-f_3 - T_2 = 0. \quad (17)$$

Notice that equations (15)-(17) imply that the condition of global force balance (4) is satisfied. Our aim now is to obtain two ODEs for L_1 and L_2 . From equations (15)-(17) we can easily express the forces as functions of T_1 and T_2 . If we plug the resulting expressions into equations (1)-(3) we obtain

$$v_1 = \frac{T_1}{6\pi\mu a} + \frac{T_2 - T_1}{4\pi\mu L_1} - \frac{T_2}{4\pi\mu(L_1 + L_2)}, \quad (18)$$

$$v_2 = \frac{T_1}{4\pi\mu L_1} + \frac{T_2 - T_1}{6\pi\mu a} - \frac{T_2}{4\pi\mu L_2}, \quad (19)$$

$$v_3 = \frac{T_1}{4\pi\mu(L_1 + L_2)} + \frac{T_2 - T_1}{4\pi\mu L_2} - \frac{T_2}{6\pi\mu a}. \quad (20)$$

These equations, combined with the kinematic relations (5) and (6), yield the following system of ODEs governing the evolution of L_1 and L_2

$$\dot{L}_1 = \frac{1}{\pi\mu} \left(\frac{1}{2L_1} - \frac{1}{3a} \right) T_1 + \frac{1}{\pi\mu} \left(\frac{1}{6a} - \frac{1}{4L_1} - \frac{1}{4L_2} + \frac{1}{4(L_1 + L_2)} \right) T_2 \quad (21)$$

$$\dot{L}_2 = \frac{1}{\pi\mu} \left(\frac{1}{6a} - \frac{1}{4L_1} - \frac{1}{4L_2} + \frac{1}{4(L_1 + L_2)} \right) T_1 + \frac{1}{\pi\mu} \left(\frac{1}{2L_2} - \frac{1}{3a} \right) T_2. \quad (22)$$

1.3 TSS with muscle-like arms

Equations (21) and (22) drive the evolution of L_1 and L_2 once T_1 and T_2 are known functions of shape and time. In this section we introduce a further element: we model the two arms of the swimmer according to Hill's active state muscle model. A schematic representation of this model is shown in Figure 2. The contractile element is composed of an active component capable of generating a tension $S(t)$ and a linear dashpot with characteristic constant B . In addition there are two linear springs, one in parallel and one in series with the contractile element, with elastic constants k_p and k_s respectively. We assume that the active components of the two arms can generate tensions $S_1(t)$ and $S_2(t)$. Let us indicate with l_i the sum of the rest lengths of the parallel and series springs in arm i ($i = 1, 2$). Tensions and lengths are related by the

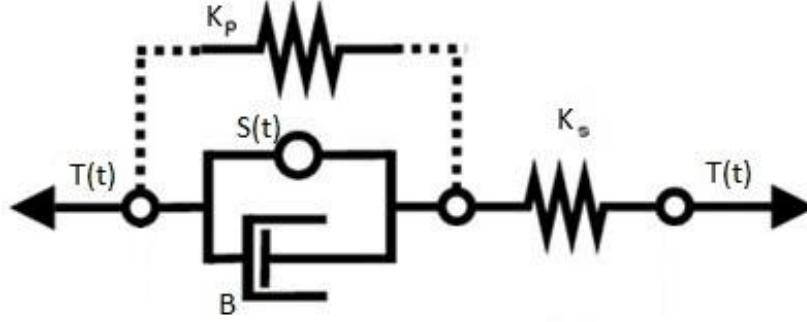


Figure 2: Hill's active state muscle model.

following equations

$$T_1 = S_1 + B_1 \dot{L}_1 - \frac{B_1}{k_{s,1}} \dot{T}_1 + k_{p,1}(L_1 - l_1) - \frac{k_{p,1}}{k_{s,1}} T_1 \quad (23)$$

$$T_2 = S_2 + B_2 \dot{L}_2 - \frac{B_2}{k_{s,2}} \dot{T}_2 + k_{p,2}(L_2 - l_2) - \frac{k_{p,2}}{k_{s,2}} T_2. \quad (24)$$

By rearranging the terms we find

$$\dot{T}_1 = -\frac{k_{s,1} + k_{p,1}}{B_1} T_1 + \frac{k_{s,1}}{B_1} S_1 + \frac{k_{s,1} k_{p,1}}{B_1} (L_1 - l_1) + k_{s,1} \dot{L}_1 \quad (25)$$

$$\dot{T}_2 = -\frac{k_{s,2} + k_{p,2}}{B_2} T_2 + \frac{k_{s,2}}{B_2} S_2 + \frac{k_{s,2} k_{p,2}}{B_2} (L_2 - l_2) + k_{s,2} \dot{L}_2. \quad (26)$$

By using equations (21) and (22) we can express \dot{L}_1 and \dot{L}_2 as functions of T_1 , T_2 , L_1 , and L_2 . Then we can plug the resulting expressions into (10), (25), and (26). As a consequence, we can rewrite (21)-(26) and (10) as a system of five ODEs governing the evolution of x , L_1 , L_2 , T_1 , and T_2 .

1.4 Non-dimensionalization

The aim of this subsection is to write the problem in non-dimensional form. We will discover that the physical parameters influence the behaviour of the dynamics through 6 non-dimensional numbers. This approach allows to obtain more general and useful results. Let $l = l_1 + l_2$ be the characteristic length of the swimmer and $1/\omega$ a characteristic time. Let us set $t^* = \omega t$, $\Lambda_i = L_i/l$, $\lambda_i = l_i/l$, $\xi = x/l$, $\alpha = a/l$, $\tau_i = T_i/(\mu\omega l^2)$, $\sigma_i = S_i/(\mu\omega l^2)$. We will indicate with the prime symbol the derivative with respect to the rescaled time t^* . Using

the new variables our system can be rewritten as

$$\Lambda'_1 = \frac{1}{\pi} \left(\frac{1}{2\Lambda_1} - \frac{1}{3\alpha} \right) \tau_1 + \frac{1}{\pi} \left(\frac{1}{6\alpha} - \frac{1}{4\Lambda_1} - \frac{1}{4\Lambda_2} + \frac{1}{4(\Lambda_1 + \Lambda_2)} \right) \tau_2 \quad (27)$$

$$\Lambda'_2 = \frac{1}{\pi} \left(\frac{1}{6\alpha} - \frac{1}{4\Lambda_1} - \frac{1}{4\Lambda_2} + \frac{1}{4(\Lambda_1 + \Lambda_2)} \right) \tau_1 + \frac{1}{\pi} \left(\frac{1}{2\Lambda_2} - \frac{1}{3\alpha} \right) \tau_2 \quad (28)$$

$$\xi' = \frac{\alpha}{6} \left(-\frac{1}{\Lambda_1 + \Lambda_2} + \frac{2}{\Lambda_2} - \frac{1}{\Lambda_1} \right) \Lambda'_1 + \frac{\alpha}{6} \left(\frac{1}{\Lambda_1 + \Lambda_2} - \frac{2}{\Lambda_1} + \frac{1}{\Lambda_2} \right) \Lambda'_2 \quad (29)$$

$$\tau'_1 = -(J_{s,1} + J_{p,1})\tau_1 + J_{s,1}\sigma_1 + J_{p,1}K_1(\Lambda_1 - \lambda_1) + K_1\Lambda'_1 \quad (30)$$

$$\tau'_2 = -(J_{s,2} + J_{p,2})\tau_2 + J_{s,2}\sigma_2 + J_{p,2}K_2(\Lambda_2 - \lambda_2) + K_2\Lambda'_2, \quad (31)$$

where the dimensionless parameters are

$$J_{s,i} := \frac{k_{s,i}}{\omega B_i}, \quad J_{p,i} := \frac{k_{p,i}}{\omega B_i}, \quad K_i := \frac{k_{s,i}}{\mu\omega l}, \quad (32)$$

for $i = 1, 2$.

1.5 TSS with one muscle-like arm and one passive elastic arm

Now we replace the tail arm with a passive elastic spring. Let us indicate with l_1 the rest length and with h the elastic constant of the spring. Equations (27)-(29) and (31) remain valid. Equation (30) is replaced by

$$\tau_1 = H(\Lambda_1 - \lambda_1), \quad (33)$$

where $\lambda_1 = l_1/l$ and $H = h/(\omega\mu l)$.

2 TSS with two muscle-like arms

In this section we present a detailed study of the TSS with two muscle-like arms. For the sake of simplicity we assume that the two arms are identical. Therefore

$$\lambda_1 = \lambda_2 = 1/2 \quad (34)$$

$$K_1 = K_2 =: K \quad (35)$$

$$J_{s,1} = J_{s,2} =: J_s \quad (36)$$

$$J_{p,1} = J_{p,2} =: J_p. \quad (37)$$

We consider the case in which the tensions developed by the active components are small, namely,

$$\sigma_i = \epsilon \tilde{\sigma}_i, \quad (38)$$

with $\epsilon \ll 1$ and $|\tilde{\sigma}_i| \leq 1$. We assume that σ_1 and σ_2 are periodic. In the first subsection we study the qualitative properties of the solutions. In the second subsection we compute the solutions analytically to leading order in ϵ . In the third subsection we present the results of numerical simulations and in the fourth one we study some optimization problems.

2.1 Qualitative properties of the solutions

In this subsection we prove that, for small enough values of ϵ , there exists one and only one periodic orbit and that this orbit is asymptotically stable. Our analysis is based on some classical results on periodically perturbed systems which can be found in [17].

We observe that in the ODEs (27)-(31), ξ does not appear in the velocity field. This is due to the fact that the response of the system is invariant under translations. As a consequence, the differential problem for ξ is decoupled from the rest. So we can restrict our attention to the four-dimensional system for $\Lambda_1, \Lambda_2, \tau_1, \tau_2$. Instead of Λ_1 and Λ_2 we use the variables $u_1 = \Lambda_1 - \lambda_1$ and $u_2 = \Lambda_2 - \lambda_2$. Let us set $Y := (u_1, u_2, \tau_1, \tau_2)^{tr}$ and $\tilde{J} := J_s + J_p$. We can write our system in the form

$$Y' = f(Y) + \epsilon g(t^*), \quad (39)$$

where $f(Y)$ is

$$\begin{pmatrix} \frac{1}{\pi} \left(\frac{1}{2(\lambda_1 + u_1)} - \frac{1}{3\alpha} \right) \tau_1 + \frac{1}{\pi} \left(\frac{1}{6\alpha} - \frac{1}{4(\lambda_1 + u_1)} - \frac{1}{4(\lambda_2 + u_2)} + \frac{1}{4(\lambda_1 + u_1 + \lambda_2 + u_2)} \right) \tau_2 \\ \frac{1}{\pi} \left(\frac{1}{6\alpha} - \frac{1}{4(\lambda_1 + u_1)} - \frac{1}{4(\lambda_2 + u_2)} + \frac{1}{4(\lambda_1 + u_1 + \lambda_2 + u_2)} \right) \tau_1 + \frac{1}{\pi} \left(\frac{1}{2(\lambda_2 + u_2)} - \frac{1}{3\alpha} \right) \tau_2 \\ J_p K u_1 + \left[\frac{K}{\pi} \left(\frac{1}{2(\lambda_1 + u_1)} - \frac{1}{3\alpha} \right) - \tilde{J} \right] \tau_1 + \frac{K}{\pi} \left(\frac{1}{6\alpha} - \frac{1}{4(\lambda_1 + u_1)} - \frac{1}{4(\lambda_2 + u_2)} + \frac{1}{4(\lambda_1 + u_1 + \lambda_2 + u_2)} \right) \tau_2 \\ J_p K u_2 + \left[\frac{K}{\pi} \left(\frac{1}{2(\lambda_2 + u_2)} - \frac{1}{3\alpha} \right) - \tilde{J} \right] \tau_2 + \frac{K}{\pi} \left(\frac{1}{6\alpha} - \frac{1}{4(\lambda_1 + u_1)} - \frac{1}{4(\lambda_2 + u_2)} + \frac{1}{4(\lambda_1 + u_1 + \lambda_2 + u_2)} \right) \tau_1 \end{pmatrix}, \quad (40)$$

and

$$g(t^*) = \begin{pmatrix} 0 \\ 0 \\ J_s \tilde{\sigma}_1(t^*) \\ J_s \tilde{\sigma}_2(t^*) \end{pmatrix}. \quad (41)$$

The unperturbed system $Y' = f(Y)$ has the equilibrium point $Y = 0$. The variational system with respect to this equilibrium point (see [17], page 303) is

$$Z' = AZ, \quad (42)$$

where

$$A := \begin{pmatrix} 0 & 0 & Q & R \\ 0 & 0 & R & Q \\ J_p K & 0 & KQ - \tilde{J} & KR \\ 0 & J_p K & KR & KQ - \tilde{J} \end{pmatrix}, \quad (43)$$

and

$$Q := \frac{1}{\pi} \left(1 - \frac{1}{3\alpha} \right) \quad (44)$$

$$R := \frac{1}{\pi} \left(\frac{1}{6\alpha} - \frac{3}{4} \right). \quad (45)$$

Now we would like to prove that all the eigenvalues of A have a negative real part. If this is true then all the characteristic multipliers of system (42) are in

modulus strictly less than one. As a consequence we can apply theorems 6.1.1 and 6.1.3 of [17] and conclude that, for small enough values of ϵ , there exists one and only one periodic orbit. Moreover, this orbit is asymptotically stable. The characteristic polynomial of A is

$$\begin{aligned} p_A(x) = x^4 + 2(\tilde{J} - KQ)x^3 + [K^2(Q^2 - R^2) + \tilde{J}^2 - 2\tilde{J}KQ - 2J_pKQ]x^2 + \dots \\ \dots + [J_pK^2(Q^2 - R^2) - 2J_pKQ\tilde{J}]x + (J_pK)^2(Q^2 - R^2). \end{aligned} \quad (46)$$

Let us indicate with a_j , $j = 0, 1, 2, 3$ the coefficients, so that

$$p_A(x) = x^4 + a_3x^3 + a_2x^2 + a_1x + a_0. \quad (47)$$

First of all we observe that $a_j > 0$ for every j . This follows from the fact that, if α is small enough, then $Q < 0$, $R > 0$, $|Q| < R$. Having all the coefficients with the same sign is a necessary condition for $p_A(x)$ to have only roots with negative real part. The assumption that α is small is a natural one, because all of our analysis is based on the hypothesis that the radius of the spheres is small compared to the lengths of the arms. The table associated to the polynomial by means of the Routh method is

$$\begin{bmatrix} 1 & a_2 & a_0 \\ a_3 & a_1 & 0 \\ b_3 & b_2 & 0 \\ c_2 & 0 & 0 \\ \dots & \dots & \dots \end{bmatrix}, \quad (48)$$

where

$$b_3 = (a_3a_2 - a_1)/a_3 \quad (49)$$

$$b_2 = a_0 \quad (50)$$

$$c_2 = (a_1b_3 - a_3b_2)/b_3. \quad (51)$$

Let us study the signs of b_3 and c_2 . Notice that

$$b_3 = a_2 - a_1/a_3 \quad (52)$$

$$= a_2 + \frac{2J_pKQ\tilde{J} - J_p(KQ)^2 + J_p(KR)^2}{2(\tilde{J} - KQ)} \quad (53)$$

$$= a_2 + \frac{J_pKQ}{2} + \frac{J_pKQ(\tilde{J} - (KR)^2/(KQ))}{2(\tilde{J} - KQ)}. \quad (54)$$

Now we notice that, since $|Q| < R$, we have

$$\tilde{J} - (KR)^2/(KQ) \leq \tilde{J} - KQ. \quad (55)$$

As a consequence,

$$b_3 \geq a_2 + J_pKQ = K^2(Q^2 - R^2) + \tilde{J}^2 - 3J_pKQ - 2J_sKQ > 0. \quad (56)$$

Notice that $\text{sign}(c_2) = \text{sign}(a_1 b_3 - a_3 b_2)$. By using (56) we see that

$$\begin{aligned} a_1 b_3 - a_3 b_2 &\geq (Q^2 - R^2)[2J_p K^4 Q^2 + 2J_p \tilde{J}^2 K^2 - 4J_p J_s K^3 Q - 6J_p^2 K^3 \tilde{J} Q] + \dots \\ &\dots - 2J_p \tilde{J} K^3 Q(Q^2 - R^2) - 2J_p \tilde{J}^3 K Q + 4(J_p K)^2 \tilde{J} Q^2 + \dots \\ &\dots + 4J_p J_s \tilde{J} (K Q)^2 + 2(\tilde{J} - K Q)(J_p K)^2 R^2 > 0. \end{aligned} \quad (57)$$

So b_3 and c_2 are both positive. Therefore we see from table (48) that there are three roots with negative real part. Since the determinant of A is positive, also the fourth root must have negative real part.

2.2 Asymptotic expansions

In this section we compute analytic expressions for the solutions, to leading order in ϵ . Let us assume that

$$\tilde{\sigma}_1 = \tilde{a}_1 \sin(t^*) + \tilde{b}_1 \cos(t^*) \quad (58)$$

$$\tilde{\sigma}_2 = \tilde{a}_2 \sin(t^*) + \tilde{b}_2 \cos(t^*), \quad (59)$$

with $|\tilde{a}_j| + |\tilde{b}_j| \leq 1$, $j = 1, 2$. We express the solutions in power series as follows

$$u_1 = \epsilon u_1^{(1)} + \epsilon^2 u_1^{(2)} + \dots \quad (60)$$

$$u_2 = \epsilon u_2^{(1)} + \epsilon^2 u_2^{(2)} + \dots \quad (61)$$

$$\tau_1 = \epsilon \tau_1^{(1)} + \epsilon^2 \tau_1^{(2)} + \dots \quad (62)$$

$$\tau_2 = \epsilon \tau_2^{(1)} + \epsilon^2 \tau_2^{(2)} + \dots \quad (63)$$

Let us set $X = (u_1^{(1)}, u_2^{(1)}, \tau_1^{(1)}, \tau_2^{(1)})^{tr}$. The problem satisfied by X is

$$\begin{cases} X' = AX + g(t^*) \\ X(0) = 0. \end{cases} \quad (64)$$

The solution of this problem can be computed with the help of Duhamel's formula

$$X(t^*) = \int_0^{t^*} e^{A(t^*-s)} g(s) ds. \quad (65)$$

However, since the exponential of A is difficult to compute, we choose a different strategy. We know from the previous subsection that the solution converges to a periodic orbit and we would like to study the stationary regime of the system. So we are not really interested in the solution of (64). Rather, we would like to compute the periodic orbit. This problem can be reduced to the problem of solving a linear system. First of all we notice that g can be rewritten as

$$g(t^*) = \hat{g}_s \sin(t^*) + \hat{g}_c \cos(t^*), \quad (66)$$

where $\hat{g}_s = (0, 0, J_s \tilde{a}_1, J_s \tilde{a}_2)^{tr}$ and $\hat{g}_c = (0, 0, J_s \tilde{b}_1, J_s \tilde{b}_2)^{tr}$. We look for a solution in the following form

$$X(t^*) = \hat{X}_s \sin(t^*) + \hat{X}_c \cos(t^*), \quad (67)$$

with $\hat{X}_s, \hat{X}_c \in \mathbb{R}^4$. Notice that $X' = -\hat{X}_c \sin(t^*) + \hat{X}_s \cos(t^*)$. So our differential equation becomes

$$-\hat{X}_c \sin(t^*) + \hat{X}_s \cos(t^*) = (A\hat{X}_s + \hat{g}_s) \sin(t^*) + (A\hat{X}_c + \hat{g}_c) \cos(t^*). \quad (68)$$

Since the equality must hold for every time t^* , we obtain the following linear system

$$\begin{cases} -\hat{X}_c = A\hat{X}_s + \hat{g}_s \\ \hat{X}_s = A\hat{X}_c + \hat{g}_c. \end{cases} \quad (69)$$

We can rewrite the problem in compact form

$$\begin{pmatrix} -A & -\mathbb{1} \\ \mathbb{1} & -A \end{pmatrix} \begin{pmatrix} \hat{X}_s \\ \hat{X}_c \end{pmatrix} = \begin{pmatrix} \hat{g}_s \\ \hat{g}_c \end{pmatrix}. \quad (70)$$

Now suppose that

$$u_1^{(1)} = a_1 \sin(t^*) + b_1 \cos(t^*) \quad (71)$$

$$u_2^{(1)} = a_2 \sin(t^*) + b_2 \cos(t^*) \quad (72)$$

$$\tau_1^{(1)} = c_1 \sin(t^*) + d_1 \cos(t^*) \quad (73)$$

$$\tau_2^{(1)} = c_2 \sin(t^*) + d_2 \cos(t^*), \quad (74)$$

namely, $\hat{X}_s = (a_1, a_2, c_1, c_2)^{tr}$ and $\hat{X}_c = (b_1, b_2, d_1, d_2)^{tr}$. The linear problem (70) corresponds to the following set of equations

$$a_1 = Qd_1 + Rd_2 \quad (75)$$

$$a_2 = Rd_1 + Qd_2 \quad (76)$$

$$b_1 = -Qc_1 - Rc_2 \quad (77)$$

$$b_2 = -Rc_1 - Qc_2 \quad (78)$$

$$c_1 + (\tilde{J} - KQ)d_1 - KRd_2 - J_p K b_1 = J_s \tilde{b}_1 \quad (79)$$

$$c_2 + (\tilde{J} - KQ)d_2 - KRd_1 - J_p K b_2 = J_s \tilde{b}_2 \quad (80)$$

$$d_1 - (\tilde{J} - KQ)c_1 + KRc_2 + J_p K a_1 = -J_s \tilde{a}_1 \quad (81)$$

$$d_2 - (\tilde{J} - KQ)c_2 + KRc_1 + J_p K a_2 = -J_s \tilde{a}_2. \quad (82)$$

The first four equations allow us to express a_1 , a_2 , b_1 , and b_2 as linear combinations of c_1 , c_2 , d_1 , and d_2 . If we plug the resulting expressions into the last four equations we obtain

$$M \begin{pmatrix} c_1 \\ c_2 \\ d_1 \\ d_2 \end{pmatrix} = J_s \begin{pmatrix} \tilde{b}_1 \\ \tilde{b}_2 \\ -\tilde{a}_1 \\ -\tilde{a}_2 \end{pmatrix}, \quad (83)$$

where

$$M = \begin{pmatrix} 1 + J_p K Q & J_p K R & \tilde{J} - K Q & -K R \\ J_p K R & 1 + J_p K Q & -K R & \tilde{J} - K Q \\ K Q - \tilde{J} & K R & 1 + J_p K Q & J_p K R \\ K R & K Q - \tilde{J} & J_p K R & 1 + J_p K Q \end{pmatrix}. \quad (84)$$

So now our problem is to check if M is invertible and to compute M^{-1} . Let us set

$$M_1 = 1 + J_p K Q \quad (85)$$

$$M_2 = J_p K R \quad (86)$$

$$M_3 = \tilde{J} - K Q \quad (87)$$

$$M_4 = K R. \quad (88)$$

Straightforward computations show that

$$\det(M) = (M_1^2 - M_2^2)^2 + (M_3^2 - M_4^2)^2 + 2(M_1 M_3 + M_2 M_4)^2 + 2(M_1 M_4 + M_2 M_3)^2. \quad (89)$$

We observe that when α is sufficiently small $|Q| > R$ and so $M_3 > M_4$. It follows that $(M_3^2 - M_4^2)^2 > 0$, thus $\det(M)$ is strictly positive. So we can compute the inverse of M , and the result is

$$M^{-1} = \frac{1}{\det M} \begin{pmatrix} m_1 & m_2 & m_3 & -m_4 \\ m_2 & m_1 & -m_4 & m_3 \\ -m_3 & m_4 & m_1 & m_2 \\ m_4 & -m_3 & m_2 & m_1 \end{pmatrix}, \quad (90)$$

where

$$m_1 := M_1^3 + 2M_2 M_3 M_4 + M_1 M_3^2 - M_1 M_2^2 + M_1 M_4^2 \quad (91)$$

$$m_2 := M_2^3 + 2M_1 M_3 M_4 + M_2 M_4^2 + M_2 M_3^2 - M_1^2 M_2 \quad (92)$$

$$m_3 := -M_3^3 - 2M_1 M_2 M_4 + M_3 M_4^2 - M_1^2 M_3 - M_2^2 M_3 \quad (93)$$

$$m_4 := -M_4^3 - 2M_1 M_2 M_3 - M_1^2 M_4 + M_3^2 M_4 - M_2^2 M_4. \quad (94)$$

Now we can compute the coefficients $a_i, b_i, c_i, d_i, i = 1, 2$. First we observe that

$$\begin{pmatrix} c_1 \\ c_2 \\ d_1 \\ d_2 \end{pmatrix} = J_s M^{-1} \begin{pmatrix} \tilde{b}_1 \\ \tilde{b}_2 \\ -\tilde{a}_1 \\ -\tilde{a}_2 \end{pmatrix}. \quad (95)$$

The remaining coefficients can be computed using (75)-(78). At steady state the shape of the system evolves along a closed loop in the configuration space. Figure 3 shows a comparison between the loops obtained through numerical simulations and the ones corresponding to the leading order approximation.

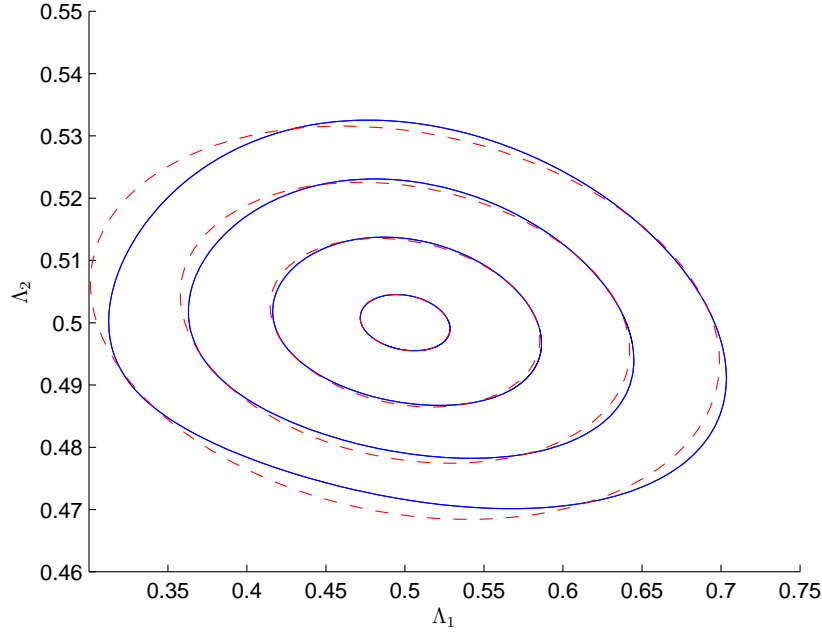


Figure 3: These curves in the configuration space are the loops along which the shape of the TSS with muscle-like arms evolves. The full blue lines show the results of numerical simulations while the red dashed lines correspond to leading order approximations. The loops in this picture are obtained by varying ϵ and choosing the other parameters as in Table 1. The different loops, from the smallest to the largest, correspond to $\epsilon = 0.1$, $\epsilon = 0.3$, $\epsilon = 0.5$, and $\epsilon = 0.7$. We see from the picture that the error becomes vanishingly small for small values of ϵ .

2.3 Numerical simulations

In this section we present the results of some numerical simulations. We used MATLAB ode45 procedure, which consists of a Runge-Kutta integration scheme with adaptive step size. The values of the dimensionless parameters used in the simulations are shown in Table 1.

J_s	J_p	K	α	\tilde{a}_1	\tilde{b}_1	\tilde{a}_2	\tilde{b}_2	ϵ
4	3	2	0.1	1	0	0.25	0	0.7

Table 1: Values of the parameters used in the numerical simulations.

In section 2.1 we proved that the system converges to a periodic orbit. This is confirmed by Figure 4 in which we see that, after relaxation, Λ_1 and Λ_2 evolve

along a closed loop. Figure 5 shows the evolution of ξ . In this simulation $(\tilde{a}_1, \tilde{b}_1)$ is proportional to $(\tilde{a}_2, \tilde{b}_2)$ (see Table 1). This means that the tensions developed in the active components of the two arms are in phase with each other. If this synchronization of the active components caused a synchronization in the length change of the two arms, we would obtain a reciprocal shape change, thus no net motion in view of the scallop theorem. As we can see from figures 4 and 5, this is not the case. This property is very interesting because it implies that the swimmer can move even if the two active components are stimulated at the same frequency. We will go back to this in the following section, where this property of the system will emerge from the formula for the leading order term of the net displacement in one period. In Figure 6 we see the evolution of τ_1 and τ_2 : also in this case the behaviour at steady state is periodic, in agreement with the results of subsection 2.1.

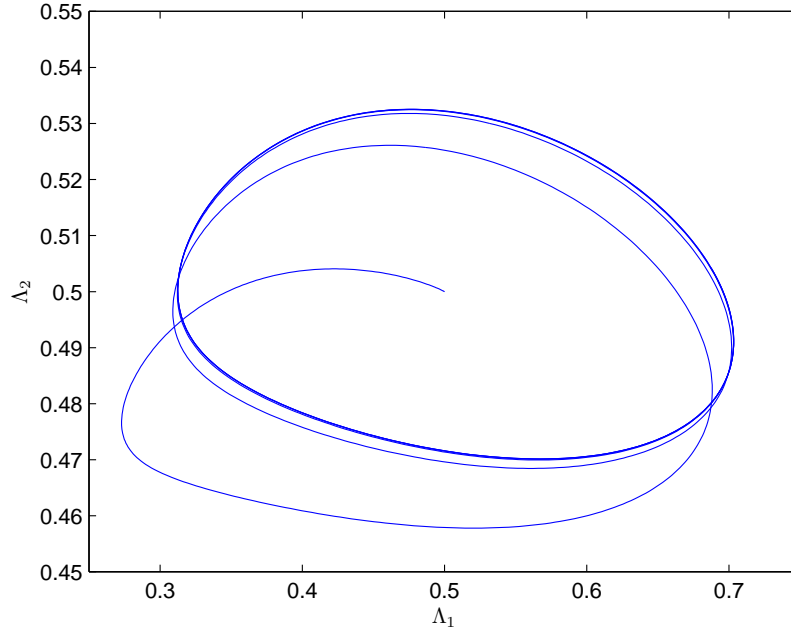


Figure 4: TSS with two mucle-like arms: evolution of the two shape parameters Λ_1 and Λ_2 . We see that the system converges to a closed loop, in agreement with the results of section 2.1.

2.4 Optimization

In this subsection we study some optimization problems. We consider three performance measures: net displacement in one period, work per travelled distance,

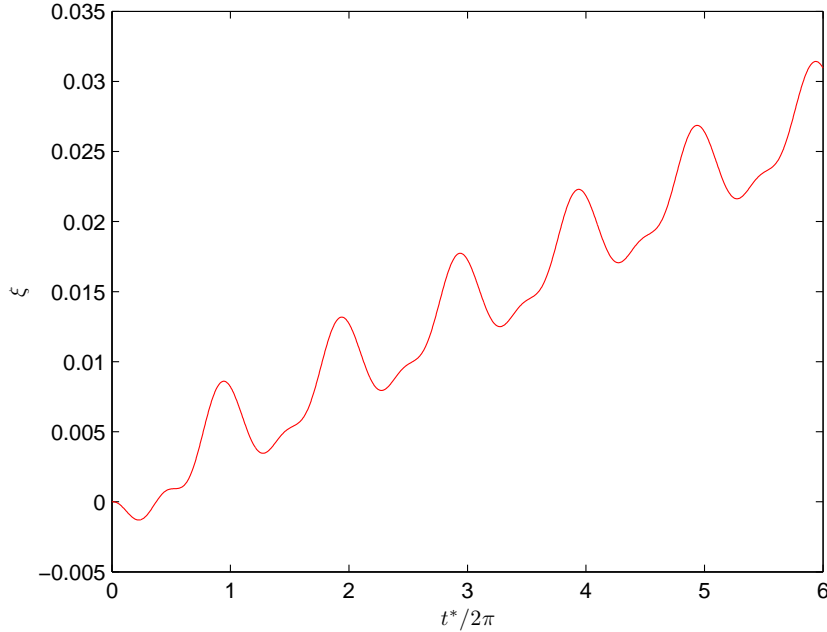


Figure 5: TSS with two muscle-like arms: plot of ξ as a function of the normalized time $t^*/2\pi$. We observe that in this case the net displacement in one period is negative.

and Lighthill's efficiency. The value of the performance measures is determined by the dimensionless parameters that appear in our system of ODEs. These parameters depend on the swimmer's body length l , on the actuation frequency ω , on the fluid viscosity μ , and on the physical constants k_s, k_p, h, B characterizing the viscoelastic arms. We consider the case in which the fluid and the swimmer are given, so that the only parameter which can be varied is the actuation frequency ω . We would like to study optimization of the different performance measures with respect to ω . Our strategy is to compute the leading order approximation of the performance measures and use the resulting expressions to study our optimization problem. Then we will compare the optimality results obtained through the leading order approximation with the outcome of numerical simulations.

The first performance measure we consider is Δx , the net displacement per period in units of body length. This quantity can be computed using formula (14). Through a simple change of integration variable we see that

$$\Delta x = \frac{\alpha}{6} \left(\frac{1}{\lambda_1^2} + \frac{1}{\lambda_2^2} - 1 \right) \int_0^{\omega T} (u_1 u_2' - u_1' u_2) dt^*. \quad (96)$$

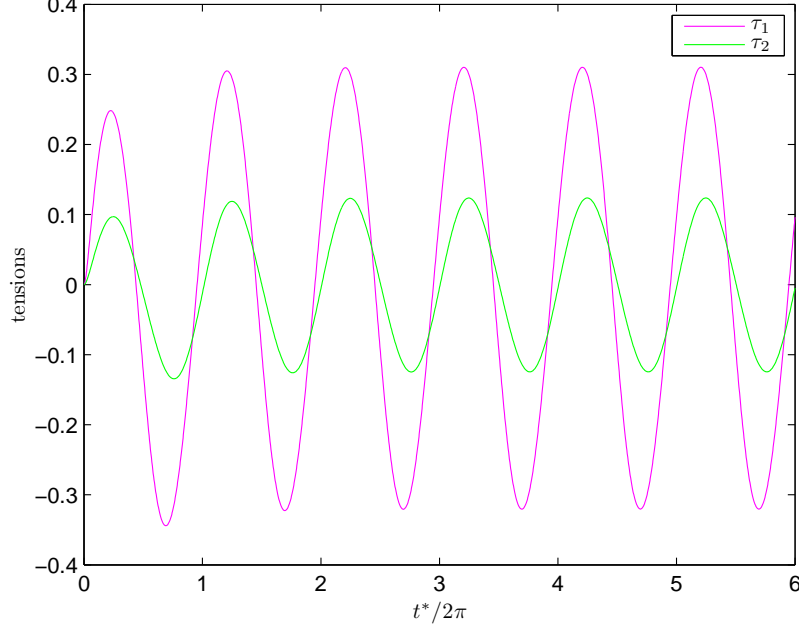


Figure 6: TSS with two muscle-like arms: plot of τ_1 and τ_2 as functions of the normalized time $t^*/2\pi$. The behaviour is periodic, in agreement with the analysis of section 2.1.

By using the leading order expressions computed above we find the following leading order approximation for Δx

$$\Delta x = \frac{7\pi\alpha}{3}(a_2b_1 - a_1b_2)\epsilon^2 + O(\epsilon^3). \quad (97)$$

By using equations (75)-(78) we obtain

$$\Delta x = \frac{7\pi\alpha}{3}(Q^2 - R^2)(c_2d_1 - c_1d_2)\epsilon^2 + O(\epsilon^3). \quad (98)$$

Now by using the expressions for c_1, c_2, d_1 and d_2 computed in subsection 2.2 we obtain

$$\frac{7\pi\alpha}{3}(Q^2 - R^2)\left(\frac{J_s}{\det M}\right)^2 \left[(m_1m_4 + m_2m_3)(\tilde{a}_2^2 + \tilde{b}_2^2 - \tilde{a}_1^2 - \tilde{b}_1^2) + (m_1^2 - m_2^2 + m_3^2 - m_4^2)(\tilde{b}_1\tilde{a}_2 - \tilde{b}_2\tilde{a}_1) \right] \epsilon^2 + O(\epsilon^3). \quad (99)$$

There are some interesting facts to point out about this formula. First of all we notice that if we change σ_1 with σ_2 and viceversa the displacement changes sign, as expected for symmetry reasons. Secondly, we observe that even in the case in which only one of the two arms is activated we obtain a non-zero displacement.

Finally, let us comment on the case in which the two active components are synchronized. Suppose there exists a constant $\eta > 0$ such that

$$\begin{pmatrix} \tilde{a}_2 \\ \tilde{b}_2 \end{pmatrix} = \eta \begin{pmatrix} \tilde{a}_1 \\ \tilde{b}_1 \end{pmatrix}. \quad (100)$$

In this case one might expect a synchronization of the length change of the two arms, leading to a reciprocal shape change which produces no net motion. However, our asymptotic analysis shows that is not the case provided that $\eta \neq 1$: from formula (99) we obtain that the leading order term of Δx is

$$\epsilon^2 \frac{7\pi\alpha}{3} (Q^2 - R^2) \left(\frac{J_s}{\det M} \right)^2 (m_1 m_4 + m_2 m_3) (\tilde{a}_1^2 + \tilde{b}_1^2) (\eta - 1) \neq 0. \quad (101)$$

Now we compute the mechanical work $\mu\omega l^3 W$ done by the active components in one period. The power expenditure $\mu\omega^2 l^3 \mathcal{P}$ is

$$\mu\omega^2 l^3 \mathcal{P} = \mu\omega^2 l^3 (\mathcal{P}_1 + \mathcal{P}_2) = S_1 \left(\frac{\dot{T}_1}{k_{s,1}} - \dot{L}_1 \right) + S_2 \left(\frac{\dot{T}_2}{k_{s,2}} - \dot{L}_2 \right). \quad (102)$$

It follows that

$$\mu\omega l^3 W = \mu\omega^2 l^3 \int_0^T \mathcal{P}(t) dt. \quad (103)$$

Using the leading order approximations computed in subsection 2.2 we find that

$$W = \pi \left[\frac{1}{K} (\tilde{b}_1 c_1 - \tilde{a}_1 d_1 + \tilde{b}_2 c_2 - \tilde{a}_2 d_2) + \tilde{a}_1 b_1 + \tilde{a}_2 b_2 - \tilde{b}_1 a_1 - \tilde{b}_2 a_2 \right] \epsilon^2 + O(\epsilon^3). \quad (104)$$

The other two performance measures we consider are the mechanical work per travelled distance

$$\zeta := \frac{W}{|\Delta x|} \quad (105)$$

and Lighthill's efficiency

$$\eta := 9\alpha \frac{\Delta x^2}{W}. \quad (106)$$

Since we have already computed leading order expressions for Δx and W , we can easily compute leading order expression for ζ and η .

Now we would like to optimize the leading order terms of the different performance measures with respect to the actuation frequency ω . First of all we will show that this problem is well-posed, namely, that each performance measure admits an optimal value of ω . Secondly, we will show that the optimality results obtained by studying the leading order approximations are in good agreement with the results of numerical simulations.

The coefficients a_i, b_i, c_i , and d_i , $i = 1, 2$, have been computed in subsection 2.2. It is not difficult to check that these coefficients are $O(1/\omega)$ when $\omega \rightarrow +\infty$ and $O(\omega)$ when $\omega \rightarrow 0$. As a consequence, it is easy to verify that

$$\begin{aligned} \Delta x^{(\text{leading order})} &= O(1/\omega^2) \text{ for } \omega \rightarrow +\infty \\ \Delta x^{(\text{leading order})} &= O(\omega^2) \text{ for } \omega \rightarrow 0. \end{aligned}$$

So the leading order expression for Δx vanishes when ω goes to zero and to $+\infty$. This implies that there exists $\omega_{\Delta x} \in (0, +\infty)$ which optimizes this performance measure. The situation is similar for the other performance measures:

$$\begin{aligned}\zeta^{(\text{leading order})} &= O(\omega^2) \text{ for } \omega \rightarrow +\infty \\ \zeta^{(\text{leading order})} &= O(1/\omega) \text{ for } \omega \rightarrow 0 \\ \eta^{(\text{leading order})} &= O(1/\omega^4) \text{ for } \omega \rightarrow +\infty \\ \eta^{(\text{leading order})} &= O(\omega^3) \text{ for } \omega \rightarrow 0.\end{aligned}$$

From these asymptotic regimes we deduce the existence of two optimal frequencies $\omega_\zeta, \omega_\eta \in (0, +\infty)$. Figures 7, 8, and 9 show plots of the different performance measures as functions of ω . Notice the existence of the optimal frequencies and the very good agreement between leading order approximations and numerical simulations.

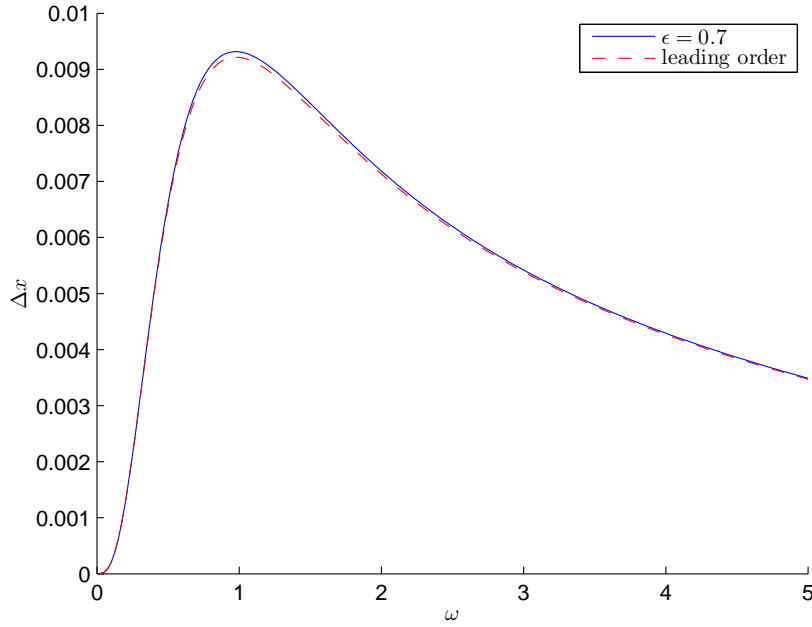


Figure 7: Net displacement per period Δx as a function of the actuation frequency ω . The blue line corresponds to the results of numerical simulations while the red dashed line corresponds to the leading order approximation. Here the values of the physical constants are such that for $\omega = 1$ the dimensionless parameters are as in Table 1.

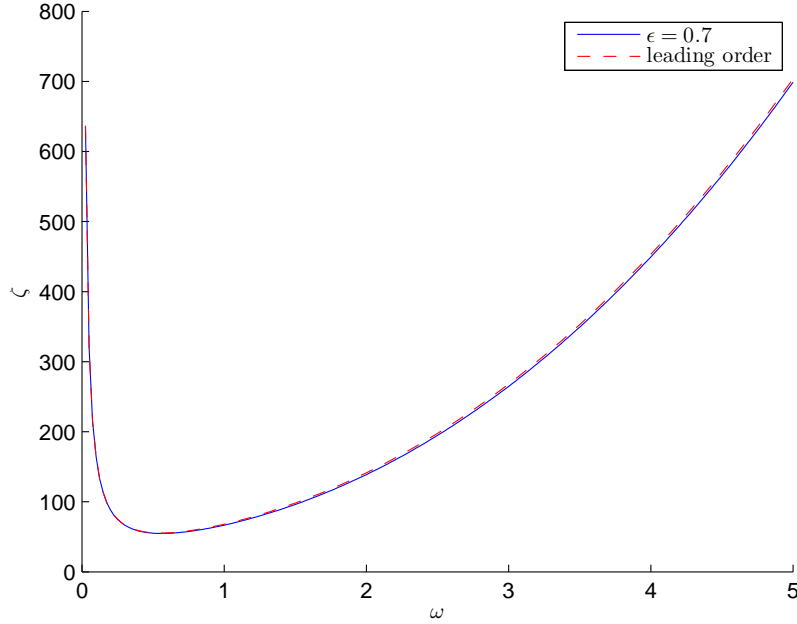


Figure 8: Work per travelled distance ζ as a function of the actuation frequency ω . The blue line corresponds to the results of numerical simulations while the red dashed line corresponds to the leading order approximation. Here the values of the physical constants are such that for $\omega = 1$ the dimensionless parameters are as in Table 1.

3 TSS with one muscle-like arm and one passive elastic arm

In this section we study the TSS with one muscle-like arm and one passive elastic arm. We assume that the active component of the muscle-like arm generates a tension

$$\sigma(t^*) = \epsilon \tilde{\sigma}(t^*), \quad (107)$$

with $\epsilon \ll 1$ and $|\tilde{\sigma}| \leq 1$. We assume that σ is a periodic function of time. In the first subsection we study the qualitative properties of the solutions. In the second subsection we compute the leading order approximation of the solutions in the asymptotic regime $\epsilon \ll 1$. In the third subsection we present the results of numerical simulations. In the fourth subsection we study some optimization problems.

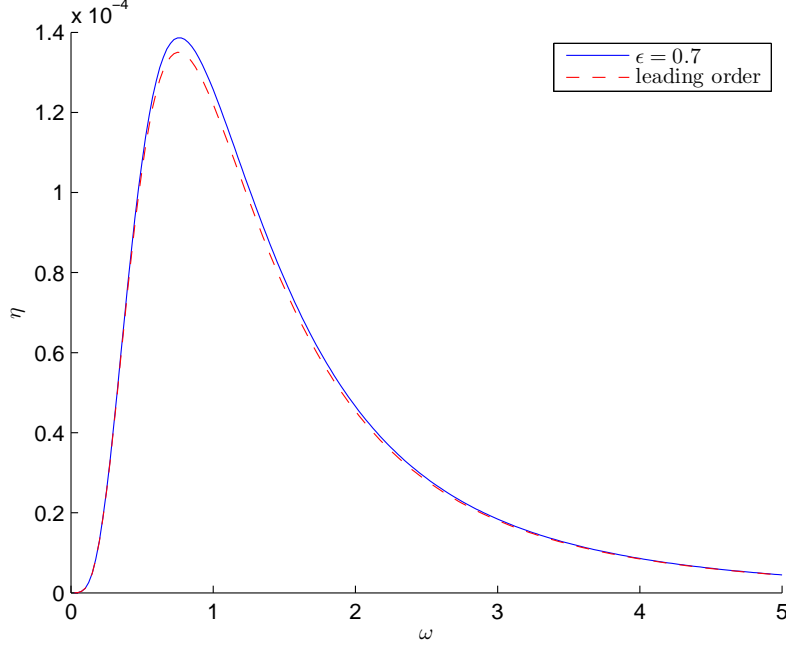


Figure 9: Lighthill's efficiency η as a function of the actuation frequency ω . The blue line corresponds to the results of numerical simulations while the red dashed line corresponds to the leading order approximation. Here the values of the physical constants are such that for $\omega = 1$ the dimensionless parameters are as in Table 1.

3.1 Qualitative properties of the solutions

For the three-sphere swimmer with one muscle-like arm and one passive elastic arm τ_1 is given by equation (33). So we can restrict our attention to the three-dimensional system of ODEs governing the evolution of the two shape variables and τ_2 . The state of the system is $Y = (u_1, u_2, \tau_2)^{tr}$ and the problem has the form

$$Y' = f(Y) + \epsilon g(t^*), \quad (108)$$

where $f(Y)$ is given by

$$\begin{pmatrix} \frac{1}{\pi} \left(\frac{1}{2(\lambda_1 + u_1)} - \frac{1}{3\alpha} \right) H u_1 + \frac{1}{\pi} \left(\frac{1}{6\alpha} - \frac{1}{4(\lambda_1 + u_1)} - \frac{1}{4(\lambda_2 + u_2)} + \frac{1}{4(\lambda_1 + u_1 + \lambda_2 + u_2)} \right) \tau_2 \\ \frac{1}{\pi} \left(\frac{1}{6\alpha} - \frac{1}{4(\lambda_1 + u_1)} - \frac{1}{4(\lambda_2 + u_2)} + \frac{1}{4(\lambda_1 + u_1 + \lambda_2 + u_2)} \right) H u_1 + \frac{1}{\pi} \left(\frac{1}{2(\lambda_2 + u_2)} - \frac{1}{3\alpha} \right) \tau_2 \\ J_p K u_2 + \left[\frac{K}{\pi} \left(\frac{1}{2(\lambda_2 + u_2)} - \frac{1}{3\alpha} \right) - \tilde{J} \right] \tau_2 + \frac{K}{\pi} \left(\frac{1}{6\alpha} - \frac{1}{4(\lambda_1 + u_1)} - \frac{1}{4(\lambda_2 + u_2)} + \frac{1}{4(\lambda_1 + u_1 + \lambda_2 + u_2)} \right) H u_1 \end{pmatrix}, \quad (109)$$

and

$$g(t^*) = \begin{pmatrix} 0 \\ 0 \\ J_p \tilde{\sigma}(t^*) \end{pmatrix}. \quad (110)$$

The unperturbed system $Y' = f(Y)$ has the equilibrium point $Y = 0$. The variational system with respect to this equilibrium point (see [17], page 303) is

$$Z' = BZ, \quad (111)$$

with

$$B = \begin{pmatrix} PH & 0 & R \\ RH & 0 & Q \\ KHR & J_p K & KQ - \tilde{J} \end{pmatrix}, \quad (112)$$

where

$$P = \frac{1}{\pi} \left(\frac{1}{2\lambda_1} - \frac{1}{3\alpha} \right) \quad (113)$$

$$Q = \frac{1}{\pi} \left(\frac{1}{2\lambda_2} - \frac{1}{3\alpha} \right) \quad (114)$$

$$R = \frac{1}{\pi} \left(\frac{1}{6\alpha} - \frac{1}{4\lambda_1} - \frac{1}{4\lambda_2} + \frac{1}{4} \right). \quad (115)$$

The characteristic polynomial of B is

$$P_B(x) = x^3 + [\tilde{J} - KQ - PH]x^2 + [KH(PQ - R^2) - P\tilde{J}H - J_p KQ]x + J_p KH(PQ - R^2). \quad (116)$$

If we prove that all the eigenvalues of B have negative real part then we can argue as in section 2.1 and conclude that, for ϵ small enough, there exists one and only one periodic orbit which is asymptotically stable. Let us call a_j , $j = 0, 1, 2$ the coefficients of the characteristic polynomial, so that

$$p_B(x) = x^3 + a_2 x^2 + a_1 x + a_0. \quad (117)$$

If α is small enough then $P < 0$, $Q < 0$, $R > 0$, $|P| < R$, and $|Q| < R$. So under this hypothesis all the coefficients of the polynomial are positive. The table associated to the polynomial by means of the Routh method is

$$\begin{bmatrix} 1 & a_1 \\ a_2 & a_0 \\ b_2 & \dots \end{bmatrix}, \quad (118)$$

with

$$b_2 = (a_1 a_2 - a_0) / a_2. \quad (119)$$

Notice that

$$\begin{aligned} a_1 a_2 - a_0 &= (\tilde{J} - KQ - PH)(KH(PQ - R^2) - P\tilde{J}H - J_p KQ) - J_p KH(PQ - R^2) \\ &= (J_s - QK - PH)(KH(PQ - R^2) - PH\tilde{J} - QKJ_p) + \dots \\ &\dots + J_p(-PH\tilde{J} - QKJ_p) > 0. \end{aligned} \quad (120)$$

It follows that $b_2 > 0$. So by applying Routh's criterion we see from table (118) that there are two roots with negative real part. Since the determinant of B is negative, also the third root must have negative real part.

3.2 Asymptotic expansions

Now we would like to compute analytically the leading order term of the solutions. Let us express the solutions in power series as follows

$$u_1 = \epsilon u_1^{(1)} + \epsilon^2 u_1^{(2)} + \dots \quad (121)$$

$$u_2 = \epsilon u_2^{(1)} + \epsilon^2 u_2^{(2)} + \dots \quad (122)$$

$$\tau_2 = \epsilon \tau_2^{(1)} + \epsilon^2 \tau_2^{(2)} + \dots \quad (123)$$

Let us set $X = (u_1^{(1)}, u_2^{(1)}, \tau_2^{(1)})^{tr}$. $X(t^*)$ is the solution of

$$\begin{cases} X' = BX + g(t^*) \\ X(0) = 0. \end{cases} \quad (124)$$

The solution of this problem can be computed with the help of Duhamel's formula. Since we are interested in the periodic behaviour of the solution at steady state, we would like to compute the periodic orbit of the system. We assume that

$$\tilde{\sigma}(t^*) = \tilde{a} \sin(t^*) + \tilde{b} \cos(t^*). \quad (125)$$

We can write g as follows

$$g(t^*) = \hat{g}_s \sin(t^*) + \hat{g}_c \cos(t^*), \quad (126)$$

where $\hat{g}_s = (0, 0, J_s \tilde{a})^{tr}$ and $\hat{g}_c = (0, 0, J_s \tilde{b})^{tr}$. We look for the periodic solution in the following form

$$X(t^*) = \hat{X}_s \sin(t^*) + \hat{X}_c \cos(t^*), \quad (127)$$

with $\hat{X}_s, \hat{X}_c \in \mathbb{R}^3$. So our differential equation becomes

$$-\hat{X}_c \sin(t^*) + \hat{X}_s \cos(t^*) = (B\hat{X}_s + \hat{g}_s) \sin(t^*) + (B\hat{X}_c + \hat{g}_c) \cos(t^*). \quad (128)$$

Since the equality must hold for every time t^* , we obtain the following linear system

$$\begin{cases} -\hat{X}_c = B\hat{X}_s + \hat{g}_s \\ \hat{X}_s = B\hat{X}_c + \hat{g}_c. \end{cases} \quad (129)$$

We can rewrite the system in compact form

$$\begin{pmatrix} -B & -\mathbb{1} \\ \mathbb{1} & -B \end{pmatrix} \begin{pmatrix} \hat{X}_s \\ \hat{X}_c \end{pmatrix} = \begin{pmatrix} \hat{g}_s \\ \hat{g}_c \end{pmatrix}. \quad (130)$$

Now suppose that

$$u_1^{(1)} = a_1 \sin(t^*) + b_1 \cos(t^*) \quad (131)$$

$$u_2^{(1)} = a_2 \sin(t^*) + b_2 \cos(t^*) \quad (132)$$

$$\tau_2^{(1)} = c \sin(t^*) + d \cos(t^*), \quad (133)$$

namely, $\hat{X}_s = (a_1, a_2, c)^{tr}$ and $\hat{X}_c = (b_1, b_2, d)^{tr}$. Let us rewrite (130) explicitly

$$PHa_1 + Rc + b_1 = 0 \quad (134)$$

$$RHa_1 + Qc + b_2 = 0 \quad (135)$$

$$a_1 - PHb_1 - Rd = 0 \quad (136)$$

$$a_2 - RHb_1 - Qd = 0 \quad (137)$$

$$-RKHa_1 - KJ_p a_2 + (\tilde{J} - KQ)c - d = J_s \tilde{a} \quad (138)$$

$$c - RKHb_1 - KJ_p b_2 + (\tilde{J} - KQ)d = J_s \tilde{b}. \quad (139)$$

From the first four equations we obtain

$$a_1 = -\frac{PRH}{1 + P^2 H^2} c + \frac{R}{1 + P^2 H^2} d \quad (140)$$

$$a_2 = RH \left(\frac{P^2 R H^2}{1 + P^2 H^2} - R \right) c + \left(Q - \frac{P R^2 H^2}{1 + P^2 H^2} \right) d \quad (141)$$

$$b_1 = \left(\frac{P^2 R H^2}{1 + P^2 H^2} - R \right) c - \frac{P R H}{1 + P^2 H^2} d \quad (142)$$

$$b_2 = \left(\frac{P R^2 H^2}{1 + P^2 H^2} - Q \right) c - \frac{R^2 H}{1 + P^2 H^2} d. \quad (143)$$

If we plug these expressions into the last two equations we obtain the following problem for c and d

$$N \begin{pmatrix} c \\ d \end{pmatrix} = J_s \begin{pmatrix} \tilde{a} \\ \tilde{b} \end{pmatrix}, \quad (144)$$

where

$$N = \frac{1}{1 + P^2 H^2} \begin{pmatrix} N_1 & -N_2 \\ N_2 & N_1 \end{pmatrix}, \quad (145)$$

and

$$N_1 = (J_p + J_s)(1 + P^2 H^2) + K H^2 (P R^2 - P^2 Q) + K H J_p R^2 - K Q \quad (146)$$

$$N_2 = 1 + H^2 P^2 + K H R^2 + K H^2 J_p (P^2 Q - P R^2) + Q K J_p. \quad (147)$$

The linear problem (130) has a solution if and only if (185) has a solution. So we need to check if N is invertible. We notice that

$$\det(N) = \frac{N_1^2 + N_2^2}{(1 + P^2 H^2)^2} > 0, \quad (148)$$

hence M is invertible. The inverse of M is given by

$$N^{-1} = \frac{1}{\det(N)} \text{cof}(N)^{tr} = \frac{1 + P^2 H^2}{N_1^2 + N_2^2} \begin{pmatrix} N_1 & N_2 \\ -N_2 & N_1 \end{pmatrix}. \quad (149)$$

Now c and d can be computed as follows

$$\begin{pmatrix} c \\ d \end{pmatrix} = J_s N^{-1} \begin{pmatrix} \tilde{a} \\ \tilde{b} \end{pmatrix}. \quad (150)$$

Once we know c and d we can compute a_1, a_2, b_1, b_2 by using equations (140)-(143). At steady state the two shape variables evolve along a closed loop in the configuration space. Figure 10 shows a comparison between the closed curves obtained through numerical simulations and the ones corresponding to the leading order approximation.

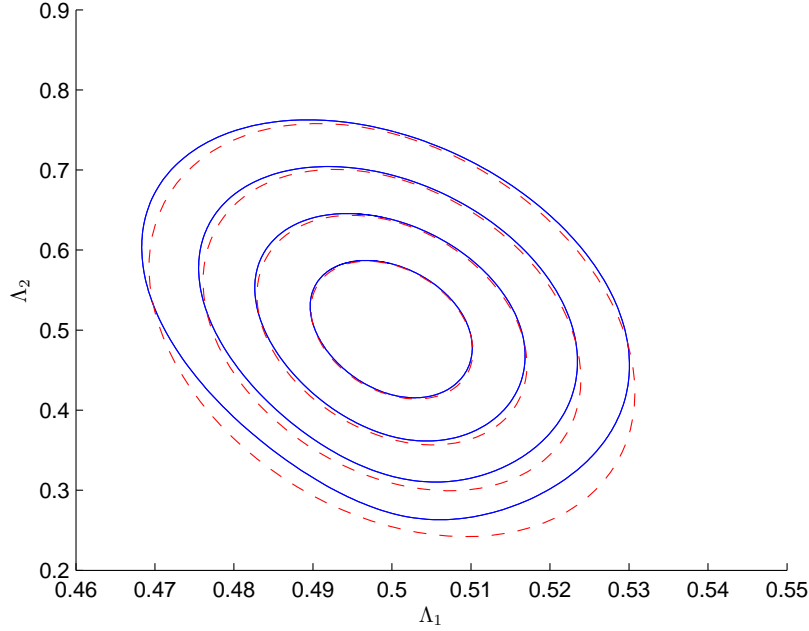


Figure 10: TSS with one muscle-like arm and one passive elastic arm: the closed curves are the loops along which the two shape parameters evolve. The full blue lines show the results of numerical simulations while the red dashed lines are the leading order approximations. These loops are obtained by varying ϵ and choosing the other parameters as in Table 2. The different loops, from the smallest to the largest, correspond to $\epsilon = 0.3$, $\epsilon = 0.5$, $\epsilon = 0.7$, and $\epsilon = 0.9$. We can see from this picture that the error becomes vanishingly small for small values of ϵ .

3.3 Numerical simulations

In this section we present the results of some numerical simulations, obtained by choosing the dimensionless parameters as in Table 2. Figure 11 shows the

J_s	J_p	K	H	α	\tilde{a}	\tilde{b}	ϵ
4	3	2	5	0.1	1	0	0.7

Table 2: Values of the parameters used in the numerical simulations.

evolution of the system in the shape space. We observe that, after relaxation, Λ_1 and Λ_2 evolve along a closed loop. In Figure 12 we see the evolution of ξ . We notice that the net displacement in one period has a negative sign, which means that the object swims with the passive arm ahead. This is a general property of the TSS with passive elastic tail. Given any periodic deformation of the active arm, it can be shown that the corresponding net displacement in one period has a negative sign [16]. Figure 13 shows a plot of τ_1 and τ_2 as functions of time. The behaviour at steady state is periodic, as expected from the results of subsection 3.1.

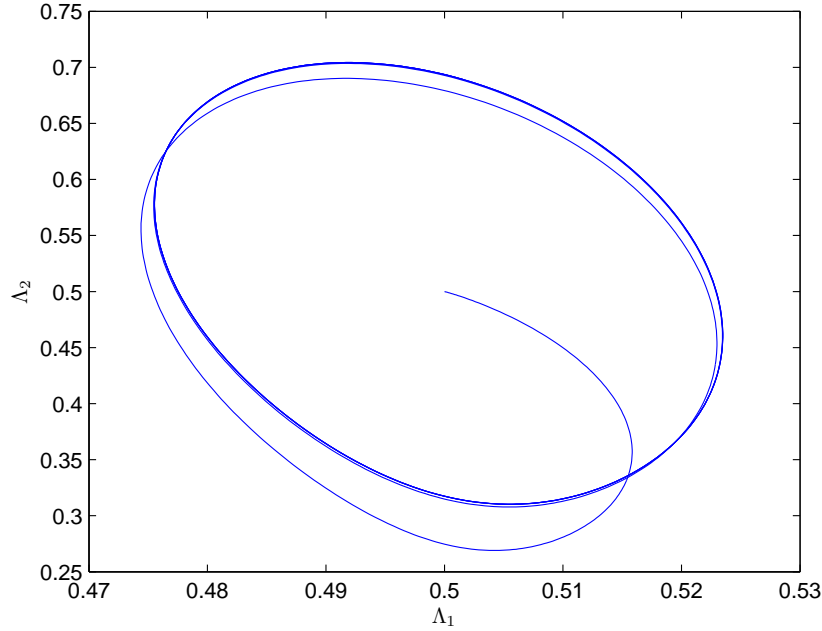


Figure 11: TSS with one muscle-like arm and one passive elastic arm: evolution of Λ_1 and Λ_2 . The solution converges to a closed loop, in agreement with the results of section 3.1.

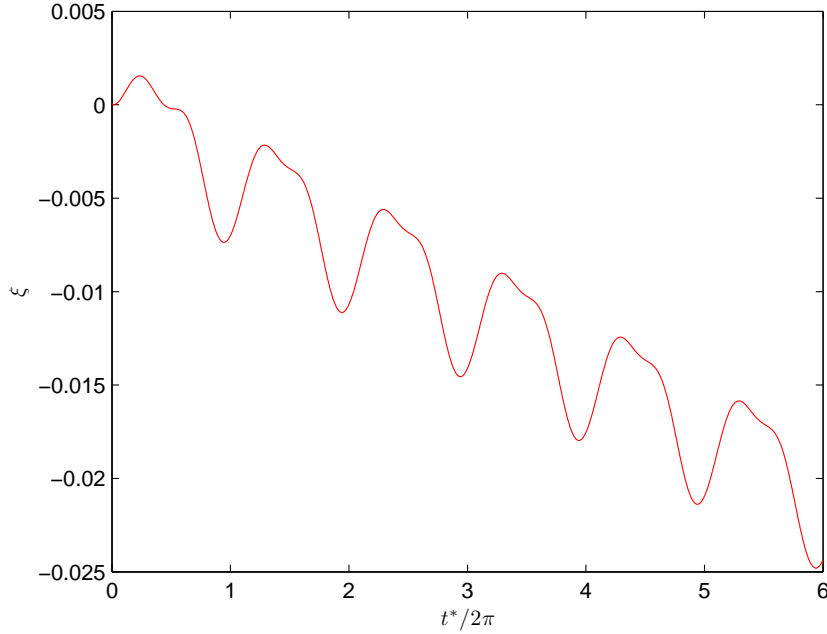


Figure 12: TSS with one muscle-like arm and one passive elastic arm: plot of ξ as a function of the normalized time $t^*/2\pi$. The net displacement in one period is negative.

3.4 Optimization

In this subsection we study some optimization problems for the three-sphere swimmer with one muscle-like arm and one passive elastic arm. The optimality measures we consider are the net displacement in one period Δx , the mechanical work per travelled distance ζ and Lighthill's efficiency η . Like in section 2.4, we assume that the fluid and swimmer are given, so that the only parameter which can be varied is the actuation frequency ω . First we study our optimization problem using the leading order approximation of the different performance measures and then we compare the results with the outcome of numerical simulations.

We start by computing the leading order expressions for the different performance measures. Formula (97) for the leading order approximation of Δx remains valid. Let us consider the mechanical work $\mu\omega l^3 W_2$ done by the active component of the muscle-like arm in one period. The power expenditure is

$$\mu\omega^2 l^3 \mathcal{P}_2 = S_2 \left(\frac{\dot{T}_2}{k_{s,2}} - \dot{L}_2 \right). \quad (151)$$

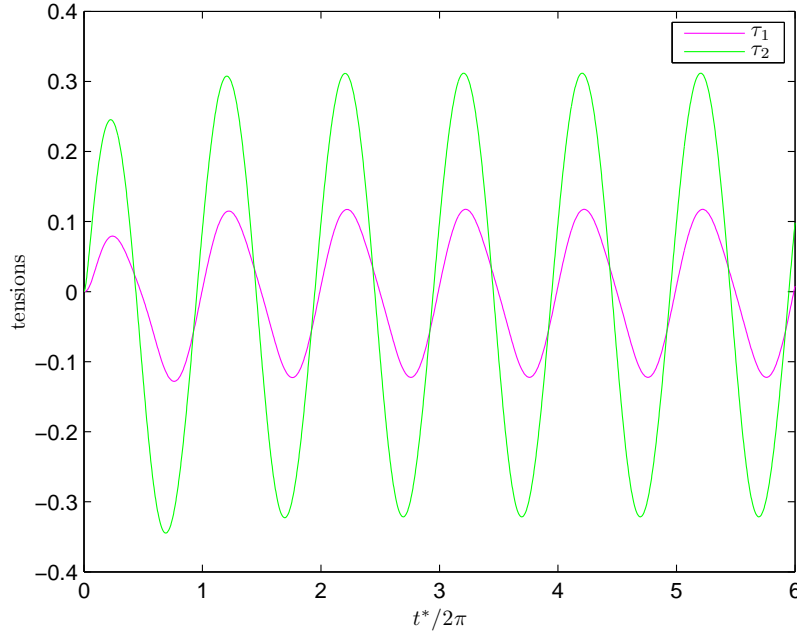


Figure 13: TSS with one muscle-like arm and one passive elastic arm: plot of τ_1 and τ_2 as functions of the normalized time $t^*/2\pi$. The behaviour is periodic, in agreement with the analysis of section 3.1.

It follows that

$$\mu\omega l^3 W_2 = \mu\omega^2 l^3 \int_0^T \mathcal{P}_2(t) dt. \quad (152)$$

So by using the results of section 3.2 we obtain

$$W = \pi \left[\frac{1}{K} (\tilde{b}c_2 - \tilde{a}d_2) + \tilde{a}b_2 - \tilde{b}a_2 \right] \epsilon^2 + O(\epsilon^3). \quad (153)$$

The work per travelled distance η and Lighthill's efficiency η are defined as in section 2.4, and the corresponding leading order approximations can be easily obtained once we know the approximation of Δx and W .

Using the formulas computed in section 3.2 it is not difficult to see that the coefficients $c, d, a_i, b_i, i = 1, 2$ are $O(1/\omega)$ when $\omega \rightarrow +\infty$ and $O(\omega)$ when $\omega \rightarrow 0$. Therefore, the asymptotic behaviour of the leading order terms of the different performance measures is exactly the same as the one observed in section 2.4. This implies existence of three optimal frequencies $\omega_{\Delta x}$, ω_ζ , and ω_η . These theoretical predictions are confirmed by Figures 14, 15, and 16. In these figures we observe the existence of the three optimal frequencies $\omega_{\Delta x}$, ω_ζ , ω_η and the high accuracy of the leading order approximations.

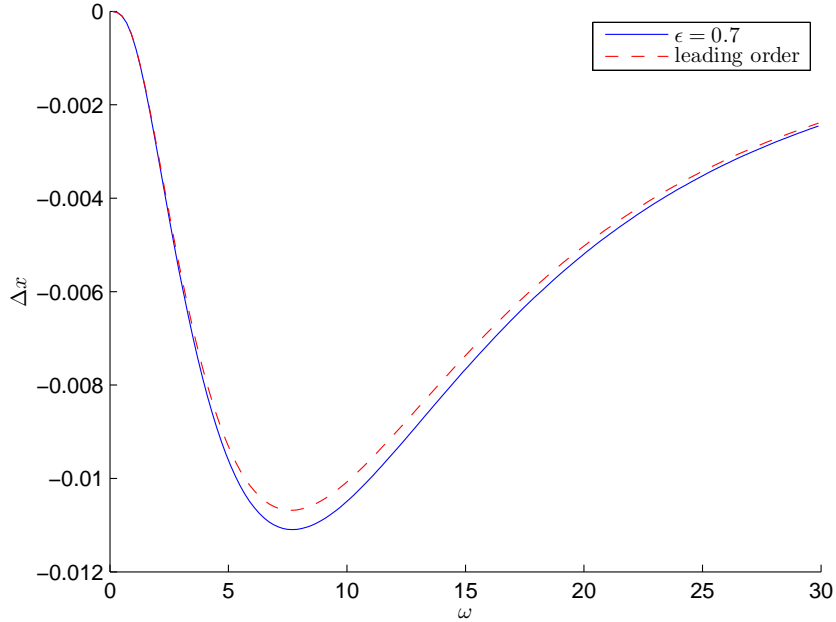


Figure 14: Net displacement per period Δx as a function of the actuation frequency ω for the TSS with one muscle-like arm and one passive elastic arm. The blue line corresponds to the results of numerical simulations while the red dashed line corresponds to the leading order approximation. Here the values of the physical constants are such that for $\omega = 1$ the dimensionless parameters are as in Table 2.

Conclusions

We studied the dynamics of the three-sphere swimmer with muscle-like arms. We assumed that the forces generated by the swimmer in the active components of the arms have intensity ϵ and vary periodically with frequency ω . We showed that the two shape parameters and the forces acting across the arms evolve according to a system of ODEs. We proved that the solutions converge to a periodic orbit. Under the assumption that $\epsilon \ll 1$, we computed the leading order approximation of the solutions at steady state. Then we studied some optimization problems. We considered three different performance measures: net displacement in one period, work per travelled distance, and Lighthill's efficiency. We studied optimization of these quantities with respect to the actuation frequency ω . We computed leading order approximations of the different performance measures. Using these approximations we showed that each performance measure admits an optimal frequency. In addition we showed that the optimality results obtained through leading order approximations are in very good

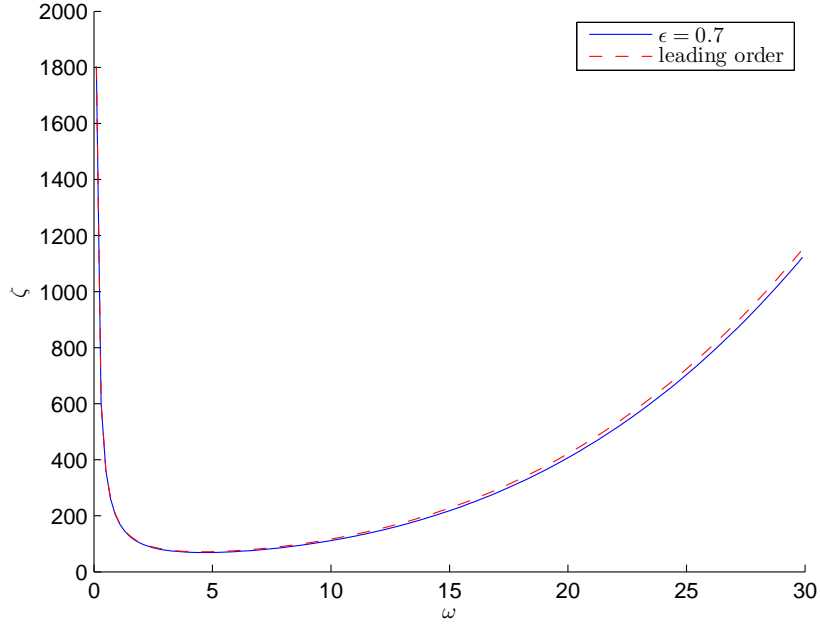


Figure 15: Work per travelled distance ζ as a function of the actuation frequency ω for the TSS with one muscle-like arm and one passive elastic arm. The blue line corresponds to the results of numerical simulations while the red dashed line corresponds to the leading order approximation. Here the values of the physical constants are such that for $\omega = 1$ the dimensionless parameters are as in Table 2.

agreement with the outcome of numerical simulations. Then we introduced the three-sphere swimmer with one muscle-like arm and one passive elastic arm. We studied this model through the same type of analysis done for the three-sphere swimmer with two muscle-like arms.

A Asymptotic expansions when the forces in the active components are generic periodic functions

A.1 TSS with two muscle-like arms

In section 2.2 we computed the leading order approximation of the solution in the case in which $\tilde{\sigma}_1$ and $\tilde{\sigma}_2$ are given by equations (58) and (59). Now we would like to consider the case in which $\tilde{\sigma}_1$ and $\tilde{\sigma}_2$ are two generic period functions

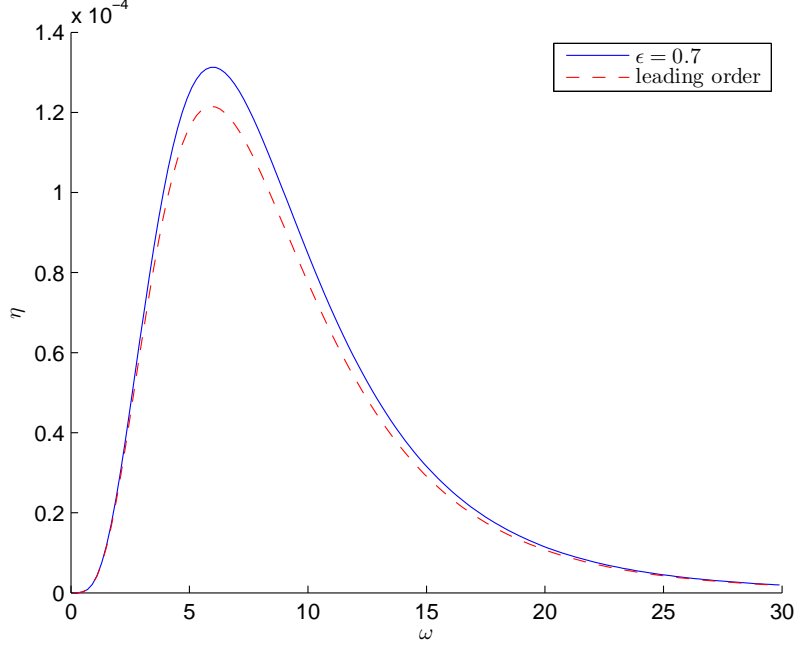


Figure 16: Lighthill's efficiency η as a function of the actuation frequency ω for the TSS with one muscle-like arm and one passive elastic arm. The blue line corresponds to the results of numerical simulations while the red dashed line corresponds to the leading order approximation. Here the values of the physical constants are such that for $\omega = 1$ the dimensionless parameters are as in Table 2.

with period 2π . We consider the expansion in Fourier series

$$\tilde{\sigma}_1(t^*) = \sum_{j=1}^{+\infty} \tilde{a}_{1,j} \sin(jt^*) + \tilde{b}_{1,j} \cos(jt^*) \quad (154)$$

$$\tilde{\sigma}_2(t^*) = \sum_{j=1}^{+\infty} \tilde{a}_{2,j} \sin(jt^*) + \tilde{b}_{2,j} \cos(jt^*) . \quad (155)$$

Let $X = (u_1^{(1)}, u_2^{(1)}, \tau_1^{(1)}, \tau_2^{(1)})^{tr}$ be the leading order term of the solution. X satisfies the differential equation

$$X' = AX + g(t^*) , \quad (156)$$

where A and g are defined as in (43) and (41) respectively. Notice that g can be written as

$$g(t^*) = \sum_{j=1}^{+\infty} \hat{g}_{s,j} \sin(jt^*) + \hat{g}_{c,j} \cos(jt^*) , \quad (157)$$

where $\hat{g}_{s,j} = (0, 0, J_s \tilde{a}_{1,j}, J_s \tilde{a}_{2,j})^{tr}$ and $\hat{g}_{c,j} = (0, 0, J_s \tilde{b}_{1,j}, J_s \tilde{b}_{2,j})^{tr}$. We are interested in computing the periodic orbit of the system, so we look for a solution in the following form

$$X(t^*) = \sum_{j=1}^{+\infty} \hat{X}_{s,j} \sin(jt^*) + \hat{X}_{c,j} \cos(jt^*), \quad (158)$$

with $\hat{X}_{s,j}, \hat{X}_{c,j} \in \mathbb{R}^4$ for every j . It is not difficult to see that the ODE (156) is equivalent to the set of linear systems

$$\begin{pmatrix} -A & -j\mathbb{1} \\ j\mathbb{1} & -A \end{pmatrix} \begin{pmatrix} \hat{X}_{s,j} \\ \hat{X}_{c,j} \end{pmatrix} = \begin{pmatrix} \hat{g}_{s,j} \\ \hat{g}_{c,j} \end{pmatrix}, \quad (159)$$

for $j \in \mathbb{N}$. Now suppose that

$$\hat{X}_{s,j} = \begin{pmatrix} a_{1,j} \\ a_{2,j} \\ c_{1,j} \\ c_{2,j} \end{pmatrix} \quad (160)$$

and

$$\hat{X}_{c,j} = \begin{pmatrix} b_{1,j} \\ b_{2,j} \\ d_{1,j} \\ d_{2,j} \end{pmatrix}. \quad (161)$$

We may rewrite (159) as follows

$$ja_{1,j} = Qd_{1,j} + Rd_{2,j} \quad (162)$$

$$ja_{2,j} = Rd_{1,j} + Qd_{2,j} \quad (163)$$

$$jb_{1,j} = -Qc_{1,j} - Rc_{2,j} \quad (164)$$

$$jb_{2,j} = -Rc_{1,j} - Qc_{2,j} \quad (165)$$

$$jc_{1,j} + (\tilde{J} - KQ)d_{1,j} - KRd_{2,j} - J_p K b_{1,j} = J_s \tilde{b}_{1,j} \quad (166)$$

$$jc_{2,j} + (\tilde{J} - KQ)d_{2,j} - KRd_{1,j} - J_p K b_{2,j} = J_s \tilde{b}_{2,j} \quad (167)$$

$$jd_{1,j} - (\tilde{J} - KQ)c_{1,j} + KRc_{2,j} + J_p K a_{1,j} = -J_s \tilde{a}_{1,j} \quad (168)$$

$$jd_{2,j} - (\tilde{J} - KQ)c_{2,j} + KRc_{1,j} + J_p K a_{2,j} = -J_s \tilde{a}_{2,j}. \quad (169)$$

Equations (162)-(165) allow us to express $a_{1,j}$, $a_{2,j}$, $b_{1,j}$, and $b_{2,j}$ as linear combinations of $c_{1,j}$, $c_{2,j}$, $d_{1,j}$, and $d_{2,j}$. If we plug the resulting expressions into the last four equations we obtain the linear problems

$$M(j) \begin{pmatrix} c_{1,j} \\ c_{2,j} \\ d_{1,j} \\ d_{2,j} \end{pmatrix} = J_s \begin{pmatrix} \tilde{b}_{1,j} \\ \tilde{b}_{2,j} \\ -\tilde{a}_{1,j} \\ -\tilde{a}_{2,j} \end{pmatrix}, \quad (170)$$

where

$$M(j) = \begin{pmatrix} j + J_p K Q / j & J_p K R / j & \tilde{J} - K Q & -K R \\ J_p K R / j & j + J_p K Q / j & -K R & \tilde{J} - K Q \\ K Q - \tilde{J} & K R & j + J_p K Q / j & J_p K R / j \\ K R & K Q - \tilde{J} & J_p K R / j & j + J_p K Q / j \end{pmatrix}. \quad (171)$$

It is not difficult to check that $M(j)$ is invertible for every $j \in \mathbb{N}$: the computations are similar to the ones done in section 2.2 for the matrix M . So we can conclude our computation with the help of the matrices $M(j)^{-1}$, $j \in \mathbb{N}$.

A.2 TSS with one muscle-like arm and one passive elastic arm

In this subsection we would like to generalize the results of subsection 3.2 by considering a more general periodic function $\tilde{\sigma}$. We assume that $\tilde{\sigma}$ is a periodic function with period 2π . We expand this function in Fourier series

$$\tilde{\sigma}(t^*) = \sum_{j=1}^{+\infty} \tilde{a}_j \sin(jt^*) + \tilde{b}_j \cos(jt^*). \quad (172)$$

Let $X = (u_1^{(1)}, u_2^{(2)}, \tau_2^{(2)})^{tr}$ be the leading order term of the solution. X satisfies the ODE

$$X' = BX + g(t^*), \quad (173)$$

where B and g are defined by equations (112) and (110) respectively. Notice that g can be written as

$$g(t^*) = \sum_{j=1}^{+\infty} \hat{g}_{s,j} \sin(jt^*) + \hat{g}_{c,j} \cos(jt^*), \quad (174)$$

where $\hat{g}_{s,j} = (0, 0, J_s \tilde{a}_j)^{tr}$ and $\hat{g}_{c,j} = (0, 0, J_s \tilde{b}_j)^{tr}$. We would like to compute the periodic orbit of the system, so we look for a solution in the form

$$X(t^*) = \sum_{j=1}^{+\infty} \hat{X}_{s,j} \sin(jt^*) + \hat{X}_{c,j} \cos(jt^*), \quad (175)$$

with $\hat{X}_{s,j}, \hat{X}_{c,j} \in \mathbb{R}^3$ for every j . The ODE (173) is equivalent to the set of linear systems

$$\begin{pmatrix} -B & -j\mathbb{1} \\ j\mathbb{1} & -B \end{pmatrix} \begin{pmatrix} \hat{X}_{s,j} \\ \hat{X}_{c,j} \end{pmatrix} = \begin{pmatrix} \hat{g}_{s,j} \\ \hat{g}_{c,j} \end{pmatrix}, \quad (176)$$

for $j \in \mathbb{N}$. Now suppose that

$$\hat{X}_{s,j} = \begin{pmatrix} a_{1,j} \\ a_{2,j} \\ c_j \end{pmatrix} \quad (177)$$

and

$$\hat{X}_{c,j} = \begin{pmatrix} b_{1,j} \\ b_{2,j} \\ d_j \end{pmatrix}. \quad (178)$$

Let us rewrite (176) explicitly

$$PHa_{1,j} + Rc_j + jb_{1,j} = 0 \quad (179)$$

$$RHa_{1,j} + Qc_j + jb_{2,j} = 0 \quad (180)$$

$$ja_{1,j} - PHb_{1,j} - Rd_j = 0 \quad (181)$$

$$ja_{2,j} - RHb_{1,j} - Qd_j = 0 \quad (182)$$

$$- RKHa_{1,j} - KJ_p a_{2,j} + (\tilde{J} - KQ)c_j - jd_j = J_s \tilde{a}_j \quad (183)$$

$$jc_j - RKHb_{1,j} - KJ_p b_{2,j} + (\tilde{J} - KQ)d_j = J_s \tilde{b}_j. \quad (184)$$

Using the first four equations we can express $a_{1,j}$, $a_{2,j}$, $b_{1,j}$, and $b_{2,j}$ as linear combinations of c_j and d_j . Then we can plug the resulting expressions into the last to equations. The result is the following linear problem

$$N(j) \begin{pmatrix} c_j \\ d_j \end{pmatrix} = J_s \begin{pmatrix} \tilde{a}_j \\ \tilde{b}_j \end{pmatrix}, \quad (185)$$

where

$$N(j) = \frac{1}{j^2 + P^2 H^2} \begin{pmatrix} N_1(j) & -N_2(j) \\ N_2(j) & N_1(j) \end{pmatrix}, \quad (186)$$

and

$$N_1(j) = (J_p + J_s)(j^2 + P^2 H^2) + KH^2(PR^2 - P^2 Q) + KHJ_p R^2/j^2 - J^2 KQ \quad (187)$$

$$N_2(j) = j^3 + jH^2 P^2 + jKHR^2 + KH^2 J_p(P^2 Q - PR^2) + j^2 QKJ_p. \quad (188)$$

A simple computation shows that $\det(N(j)) > 0$ for every j . So with the help of the matrices $N(j)^{-1}$ we can compute the coefficients of our leading order approximation.

Acknowledgments

Support by the European Research Council through the ERC Advanced Grant 340685-MicroMotility is gratefully acknowledged.

References

- [1] A. Najafi and R. Golestanian. Simple swimmer at low Reynolds number: three linked spheres. *Phys. Rev. E*, 69:062901, Jun 2004.
- [2] R. Golestanian and A. Ajdari. Analytic results for the three-sphere swimmer at low Reynolds number. *Phys. Rev. E*, 77:036308, Mar 2008.

- [3] E.M. Purcell. Life at low Reynolds number. *American Journal of Physics*, 45(1), 1977.
- [4] L.E. Becker, S.A. Koehler, and H.A. Stone. On self-propulsion of micro-machines at low Reynolds number: Purcell’s three-link swimmer. *Journal of Fluid Mechanics*, 490:15–35, 2003.
- [5] J.E. Avron, O. Kenneth, and D.H. Oaknin. Pushmepullyou: an efficient micro-swimmer. *New Journal of Physics*, 7(1):234, 2005.
- [6] J.E. Avron, O. Gat, and O. Kenneth. Optimal swimming at low Reynolds numbers. *Phys. Rev. Lett.*, 93:186001, Oct 2004.
- [7] D. Tam and A.E. Hosoi. Optimal stroke patterns for Purcell’s three-link swimmer. *Phys. Rev. Lett.*, 98:068105, Feb 2007.
- [8] F. Alouges, A. DeSimone, L. Giraldi, and M. Zoppello. Self-propulsion of slender micro-swimmers by curvature control: N-link swimmers. *International J. of Non-Linear Mechanics*, 56:132–141, 2013.
- [9] F. Alouges, A. DeSimone, and A. Lefebvre. Optimal strokes for low Reynolds number swimmers : an example. *Journal of Nonlinear Science*, 18:277–302, 2008.
- [10] F. Alouges, A. DeSimone, and A. Lefebvre. Optimal strokes for axisymmetric microswimmers. *The European Physical Journal E*, 28(3):279–284, 2009.
- [11] F. Alouges, A. DeSimone, and L. Heltai. Numerical strategies for stroke optimization of axisymmetric microswimmers. *Mathematical Models and Methods in Applied Sciences*, 21(02):361–387, 2011.
- [12] F. Alouges, A. DeSimone, L. Heltai, A. Lefebvre, and B. Merlet. Optimally swimming Stokesian robots. *Discrete and Continuous Dynamical Systems Series B*, 18, 2013.
- [13] A. DeSimone, F. Alouges, L. Heltai, and A. Lefebvre. *Natural Locomotion in Fluids and on Surfaces: Swimming, Flying and Sliding*, chapter Computing optimal strokes for low Reynolds number swimmers, pages 177–184. Springer, 2012.
- [14] S. Günther and K. Kruse. A simple self-organized swimmer driven by molecular motors. *EPL (Europhysics Letters)*, 84(6):68002, 2008.
- [15] E. Passov and Y. Or. Dynamics of Purcell’s three-link microswimmer with a passive elastic tail. *The European Physical Journal E*, 35(8), 2012.
- [16] A. Montino and A. DeSimone. Three-sphere low Reynolds number swimmer with a passive elastic arm. *European Journal of Physics E*, 2015.
- [17] M. Farkas. *Periodic Motions*. Applied Mathematical Sciences. Springer New York, 1994.